View metadata, citation and similar papers at core.ac.uk
brought to you by CORE
provided by Research Archive of Indian Institute of Technology Hyderabad

Canadian Chemical Transactions
ISSN 2291-6458 (Print), ISSN 2291-6466 (Online)
Year 2014 | Volume 2 | Issue 1 | Page 72-82

Research Article

DOI:10.13179/canchemtrans.2014.02.01.0069

Structural and Mechanistic Insights of Substituted Perimidine - Experimental and Computational Studies

Srinivas Anga, Sohag Biswas, Ravi K. Kottalanka, Bhabani S. Mallik* and Tarun K. Panda*

Department of Chemistry, Indian Institute of Technology Hyderabad, Ordnance Factory Estate, Yeddumailaram 502205, Andhra Pradesh, India.

Corresponding Author, E-mail: B. S. M bhabani@iith.ac.in, T. K. P. tpanda@iith.ac.in, Tel: + 91(40) 2301 6036, Fax: + 91(40) 2301 6032

Received: *November 23, 2013* ***Revised:*** *December 16, 2013* ***Accepted:*** *December 17, 2013* ***Published:*** *December 18, 2013*

Abstract: We report here the synthesis of phenyl(2-phenyl-2,3-dihydro-1H-perimidin-2-yl)methanone (**2**) by the condensation reaction between 1,8-diaminonaphthalene (**1**) and benzil in equimolar ratio at ambient temperature. Further reaction of compound **2** with one equivalent of sodium borohydride at 0 ºC resulted in quantitative conversion of ketone to corresponding alcohol, namely, phenyl(2-phenyl-2,3-dihydro-1H-perimidin-2-yl)methanol (**3**). The solid-state structures of both the compounds were established using single-crystal X-ray diffraction analysis. We probed, using quantum mechanics, the mechanism of formation of compound **2** through two of the most plausible routes and observed that it was more plausible that the first route, energy-wise, would result in product **2**. We also calculated the stabilization energy of intermolecular hydrogen bonding, which leads to the formation of a dimer, which has already been observed in the solid-state structure of compound **3**.

Keywords: Perimidine; Heterocyclic; Transition State; Density Functional Theory; X-Ray; Hydrogen Bonding

1. INTRODUCTION

Nitrogen-containing heterocycles are ubiquitous in nature and exhibit diverse and important biological activities [1]. Perimidines are a very interesting class of compounds that are unusual among azines in that a lone pair of pyrrole-like nitrogen atoms participate in the π system of the molecule, and there is a transfer of electron density from the heterocycle to the naphthalene ring [2–5] These perinaphtho-fused pyrimidines therefore have the characteristics of both π-deficient and π-excessive systems [6]. They have long been used in dyes and in the manufacture of polyester fibres, and more recently as the source of a novel carbene ligand [7]. Their biological activity has also attracted attention; for example, their potential to act as anti-fungal, anti-microbial, anti-ulcer and anti-tumour agents [2,8,9]. In the past, various synthetic routes were used to prepare perimidine compounds [10,11]. Very recently, Shaabani *et al.* reported the synthesis of 2,3 dihydro-1*H*-perimidine from α-hydroxy ketone and 1,8-

ISSN 2291-6458 (Print), ISSN 2291-6466 (Online)
Year 2014 | Volume 2 | Issue 1 | Page 72-82

diaminonaphthalene in the presence of cerium ammonium nitrate (CAN) catalyst [12]. Mobinikhaledi *et al.* reported the use of a zeolite catalyst to prepare a wide variety of perimidines through the cyclocondensastion reaction of 1,8-diaminonaphthalene and corresponding aromatic aldehydes [13]. Patton *et al.* also contributed to the synthesis of perimidines using 1,8-diaminonaphthalene and benzonitrile oxide. However, they did not report a structure [14]. The structures of 1-methyl-1*H*-perimidin-2(3H)-one and 1,3-dimethyl-I*H*-perimidin-2(3H)-one were reported by Claramunt *et al*. [15] Another example of 2-methylsulfanyl-1H-perimidin-3-ium iodide was reported by Ghorbani [16]. However, mechanistic details are not available for the formation of perimidines or their derivatives. Thus, there is scope for development in this field, in order to understand various routes of synthesis, using results of experiments as well as density functional theory (DFT) calculations.

Here, we report the synthesis and structures of two perimidines, phenyl(2-phenyl-2,3-dihydro-1H-perimidin-2-yl)methanone (**2**) and phenyl(2-phenyl-2,3-dihydro-1H-perimidin-2-yl)methanol (**3**) without the use of any catalyst. We also elucidate mechanistic details using DFT calculations to show the most plausible route, energy-wise, for the formation of compound **2** and stabilization energy of compound **3** due to intra-molecular hydrogen bonding.

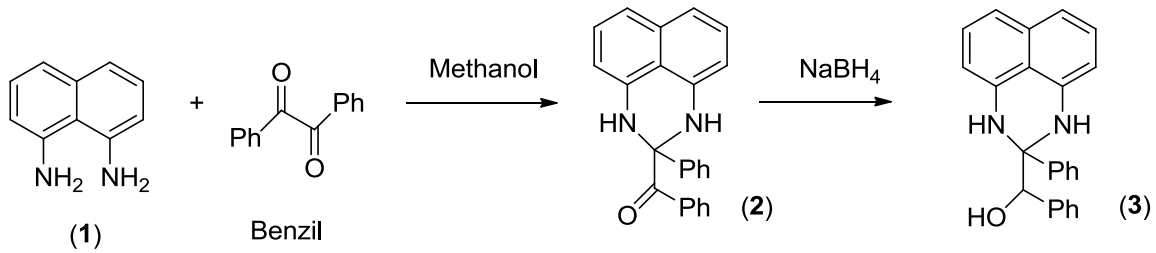

Scheme 1. Synthesis of compounds **2** and **3**

2. EXPERIMENTAL AND COMPUTATIONAL METHODS

2.1. General Information

All manipulations were done in the presence of air and moisture. ^{1}H NMR (400 MHz), ^{13}C{^{1}H} spectra were recorded on a BRUKER AVANCE III-400 spectrometer. A BRUKER ALPHA FT-IR was used for FT-IR measurement. Elemental analyses were performed on a BRUKER EURO EA at the Indian Institute of Technology Hyderabad. Starting materials 1,8-diaminonaphthalene (**1**), benzil and sodium borohydride were purchased from commercially available sources and used as such without further purification.

2.2. Synthesis of Compound 2

In a 100 mL round-bottom flask 40 mL methanol was added to a mixture of benzil (2.6 g, 12.65 mmol) and 1,8-diaminonaphthalene (2 g, 12.65 mmol) and stirred at ambient temperature for four hours. The yellow precipitate was filtered and washed with cold methanol (5 mL) and dried under vacuum. Yield 3.2 gm (73%). mp: 172 ºC. FT-IR (selected frequency): ν = 3390 (NH), 3035, 1674 (C=O), 1598, 1435, 1225, 756 cm^{-1}; 1H NMR (400 MHz, $CDCl_3$): δ = 7.69-7.71 (m, 2H, An-*H*), 7.40-7.49 (m, 6H, Ar-*H*), 7.26-7.30 (m, 2H, An*H*), 7.16-7.20 (m, 2H, Ar*H*), 6.47-6.49 (dd, 2H, An*H*), 5.22 (br, 2H, N*H*); ^{13}C{^{1}H} NMR (100 MHz, $CDCl_3$, selected resonances): δ = 201.0 (*C*=O), 140.1, 139.2, 135.5, 134.4, 132.3, 129.4, 128.6, 128.5, 127.0, 126.2, 118.0, 112.0, 106.3. Elemental analysis calcd (%) for $C_{24}H_{18}N_2O$ (350.41): C 82.26, H 5.18, N 7.99; found: C 81.90, H 5.01, N 7.72.

ISSN 2291-6458 (Print), ISSN 2291-6466 (Online)
Year 2014 | Volume 2 | Issue 1 | Page 72-82

Table 1. Crystallographic Details of Perimidines 2 and 3

Crystal	2	3
CCDC No.	967752	967753
Empirical formula	$C_{24}H_{18}N_2O$	$C_{24}H_{20}N_2O$
Formula weight	350.40	352.42
T (K)	150(2)	150(2)
λ (Å)	1.54184	0.71069
Crystal system	Monoclinic,	Triclinic
Space group	*P 21/n*	*P -1*
a (Å)	a = 5.9198(2)	10.2242(10)
b (Å)	b = 16.4914(6)	13.5627(16)
c (Å)	c = 18.2065(7)	14.8078(15)
α (^{o})	90	112.639(10)
β (^{o})	98.311	91.403(5)
γ (^{o})	90	97.631(9)
V (Å^3)	1758.76(11)	1832.8(3)
Z	4	4
D_{calc} mg/cm^{-3}	1.323	1.277
μ (mm^{-1})	0.641	0.616
F (000)	736	744
Theta range for data collection	3.63 to 70.83 deg	3.31 to 62.50 deg.
Limiting indices -	-6<=h<=7,	-11<=h<=9,
	-20<=k<=18,	-15<=k<=14,
	-22<=l<=16	-16<=l<=17
Reflections collected / unique	6751 / 3309	10793 / 5574
	[R(int) = 0.0264]	[R(int) = 0.039]
Completeness to theta = 71.25	97.6 %	95.5 %
Absorption correction	Semi-Empirical	Semi-Empirical
Max. and min. transmission	1.00000 and 0.92274	1.00000 and 0.72006
Refinement method	Full-matrix	Full-matrix
	least-squares on F^2	least-squares on F^2
Data / restraints / parameters	3309 / 0 / 244	5574 / 0 / 496
Goodness-of-fit on F^2	1.057	1.164
Final R indices [I>2sigma(I)]	R1 = 0.0538,	R1 = 0.0661,
	wR2 = 0.1404	wR2 = 0.1874
R indices (all data)	R1 = 0.0682,	R1 = 0.0970,
	wR2 = 0.1565	wR2 = 0.2562
Absolute structure parameter		
Largest diff. peak and hole	0.515 and -0.477e.A^{-3}	0.602 and -0.690 e.A^{-3}

ISSN 2291-6458 (Print), ISSN 2291-6466 (Online)
Year 2014 | Volume 2 | Issue 1 | Page 72-82

2.3. Synthesis of Compound 3

To a methanol solution (10 mL) of compound **1** (0.25 g, 0.71 mmol), $NaBH_4$ (0.053 g, 1.42 mmol) was added at 0–5 ºC. Reaction was monitored by TLC; after completion of reaction, quenched by water, the white precipitate was filtered and purified by column chromatography on silica gel (100–200 mesh), 5% petroleum ether and ethyl acetate as eluent. Yield 0.24 g (95%). mp: 164 ºC. FT-IR (selected frequency): ν = 3350 (OH) 3215(NH), 3045, 3030, 2921, 1597, 753 cm^{-1}; 1H NMR (400 MHz, $CDCl_3$): δ =7.00-7.21 (m, 12H, An-*H* and Ar-*H*), 6.84-6.86 (t, 2H, Ar*H*), 6.47-6.52 (dd, 2H, An*H*), 5.03 (br, 2H, N*H*) 4.95(s, 1H, C*H*), 3.22 (br, 1H, O*H*); $^{13}C\{^1H\}$ NMR (100 MHz, $CDCl_3$, selected resonances): δ = 141.2, 139.4, 139.4, 137.2, 134.4, 128.4, 127.9, 127.8, 127.7, 127.3, 127.0, 126.9, 118.1117.7, 114.3, 107.2, 107.0, 79.2, 73.2. Elemental analysis calcd (%) for $C_{24}H_{20}N_2O$ (352.43): C 81.79, H 5.72, N 7.95; found: C 80.97, H 5.33, N 7.62.

2.4. Single-Crystal X-Ray Structure Determinations

Single crystals of compounds **2** and **3** were grown from dichloromethane at -4 °C. In each case a crystal of suitable dimensions was mounted on a CryoLoop (Hampton Research Corp.) with a layer of light mineral oil. All measurements were made on an Agilent Supernova X-Calibur Eos CCD detector with graphite-monochromatic Cu-Kα (1.54184 Å) radiation. Crystal data and structure refinement parameters are summarized in Table 1. The structures were solved by direct methods (SIR92) [17] and refined on F^2 by the full-matrix least-squares method, using SHELXL-97 [18]. Non-hydrogen atoms were anisotropically refined. Hydrogen atoms were included in the refinement on calculated positions riding on their carrier atoms. The function minimized was $[\sum w(Fo^2 - Fc^2)^2]$ ($w = 1 / [\sigma^2 (Fo^2) + (aP)^2 + bP]$), where $P = (\mathrm{Max}(Fo^2,0) + 2Fc^2) / 3$ with $\sigma^2(Fo^2)$ from counting statistics. The function R_1 and wR_2 were $(\Sigma||Fo| - |Fc||) / \Sigma|Fo|$ and $[\Sigma w(Fo^2 - Fc^2)^2 / \Sigma(wFo^4)]^{1/2}$ respectively. The ORTEP-3 program was used to draw the molecule. Crystallographic data (excluding structure factors) for the structures reported in this paper have been deposited with the Cambridge Crystallographic Data Centre as a supplementary publication no. CCDC 967752 (**2**) and 967753 (**3**). Copies of the data can be obtained free of charge on application to CCDC, 12 Union Road, Cambridge CB21EZ, UK (fax: + (44)1223-336-033; e-mail: deposit@ccdc.cam.ac.uk).

2.5 Computational Details

The computational calculations set out in this paper were performed with the Gaussian 09 [19] suite of programs to investigate the plausible mechanisms of formation of product **2**. Based on the mechanisms shown in Scheme 2, reactants: 1,8-diaminonaphthalene (**R1**) and diketone (**R2**), each possible intermediate and product **2** were analysed by developing static models on the basis of two different levels of theories. Visualization of the models and analysis of the results obtained from Gaussian 09 were done using the Gauss view package [20]. The two pathways leading to same perimidine product, along with the reactants involved and intermediates, are shown in Figure 3. The most important part of model chemistry is to choose the appropriate method and basis set for calculations. Since our model entities contain floppy groups, we have used two different methods for our calculations. We have followed the procedure of performing higher-level total energy calculations with a geometry optimized at a lower level of theory. DFT, using the three parameter functional proposed by Becke, with correlation energy according to the Lee–Yang–Parr formula, denoted as B3LYP [21] with a 6-311+G(2d,p) basis set was used for the higher level, and Hartree-Fock (HF) method with a smaller basis set, 3-21G(d), was used for the lower level. It was determined that this method, compared to experimental results of the so-called G2 molecule set, has a reasonable maximum absolute deviation value, and energies computed with the B3LYP functional are generally insensitive to the geometry optimization level [22].

ISSN 2291-6458 (Print), ISSN 2291-6466 (Online)
Year 2014 | Volume 2 | Issue 1 | Page 72-82

Initially, structural optimization was carried out through the HF method, followed by harmonic frequency calculations, confirming that the obtained structures correspond to the minima on the potential energy surface. The single-point electronic energy was calculated using the B3LYP method for each chemical entity by taking the optimized structure. The final stabilization energy includes B3LYP single-point calculation energy with addition of zero-point energy and thermal energetics corrections obtained from the HF method. As the final crystal structure from the experiment is a dimer, we also calculated stabilization energy due to dimerization of compound **2** in the same manner, by considering the corrected energy of the monomer.

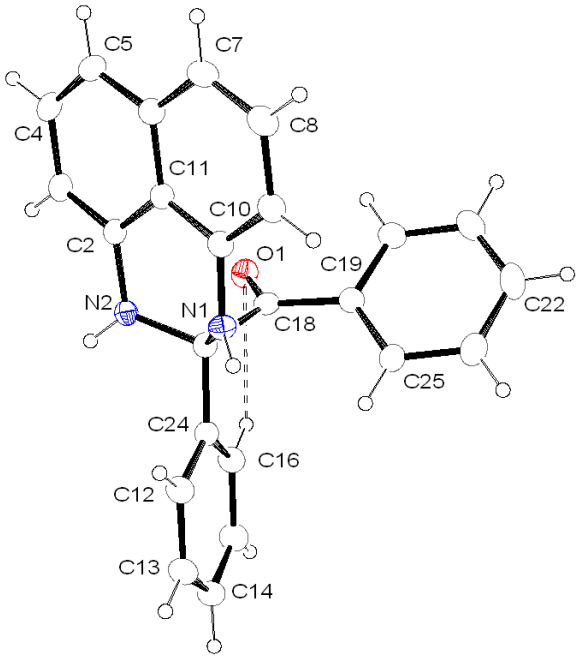

Figure 1. ORTEP diagram of **2** with thermal displacement parameters drawn at the 30% probability level. Selected bond lengths [Å] and bond angles [°]: C(1)-N(1) 1.448(2), C(1)-N(2) 1.470(2), C(1)-C(24) 1.522(3), C(1)-C(18) 1.575(3), C(2)-N(2) 1.417(2), C(10)-N(1) 1.390(2), C(18)-O(1)1.217(2), N(1)-C(1)-N(2) 106.97(15), N(1)-C(1)-C(24) 111.42(15), N(2)-C(1)-C(24) 110.05(15), N(1)-C(1)-C(18) 110.19(15), N(2)-C(1)-C(18) 109.07(15), O(1)-C(18)-C(19) 119.84(17), O(1)-C(18)-C(1) 119.79(17)

3. RESULTS AND DISCUSSION

3.1 Characterization

The substituted perimidine (compound **2**) was synthesized in the absence of any catalyst with a good yield by a condensation reaction involving 1,8-diaminonaphthalene and benzil in 1:1 molar ratio at ambient temperature. The compound was recrystallized from dichloromethane at -4 ºC (see Scheme 1). The compound phenyl(2-phenyl-2,3-dihydro-1H-perimidin-2-yl)methanol (**3**) was obtained in good yield by the reaction of compound **2** and sodium borohydride at 0 ºC (see Scheme 1). The spectroscopic and analytical data for compound **2** is consistent with the reported values. Compound **3** was characterized using spectroscopic/analytical techniques. The solid-state structures of compounds **2** and **3** were established by single-crystal X-ray diffraction analysis.

The NMR spectroscopic data for compound **2** is already reported in the literature.[12] The formation of compound **3** from compound **2** was followed by ^{1}H NMR spectra. In ^{1}H NMR spectra, two broad singlets at 5.03 ppm and 3.22 ppm and a sharp singlet at 4.95 ppm were observed. These values can

ISSN 2291-6458 (Print), ISSN 2291-6466 (Online)
Year 2014 | Volume 2 | Issue 1 | Page 72-82

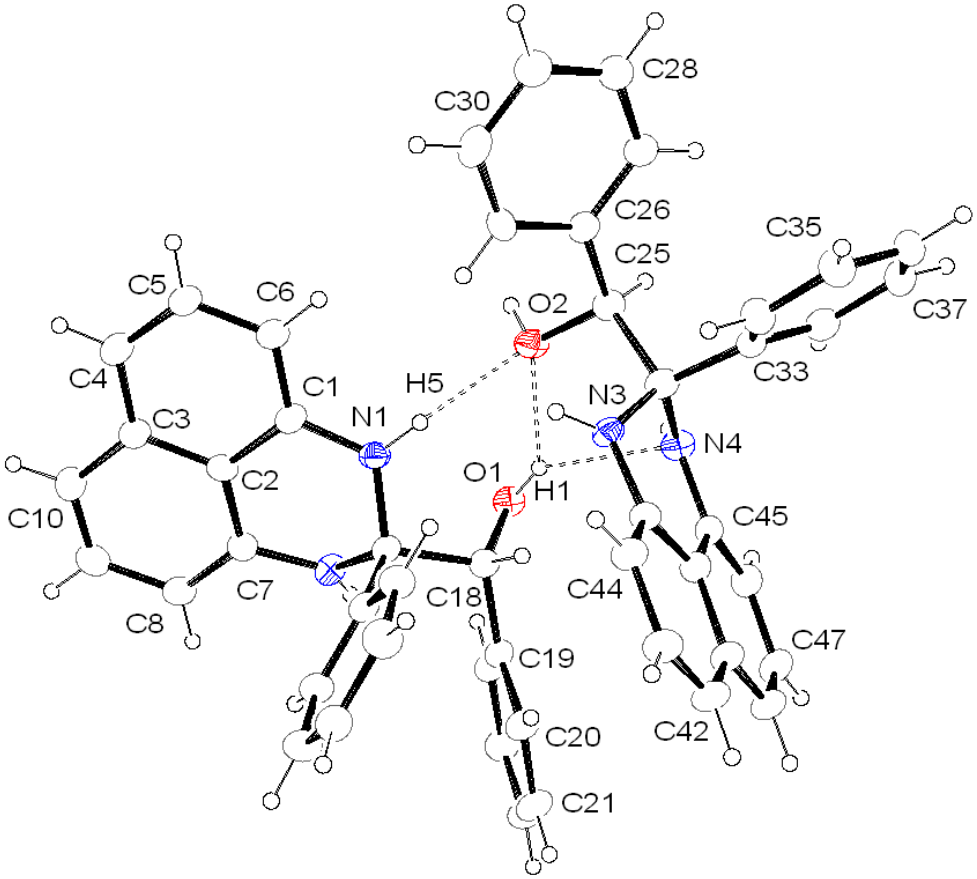

Figure 2. ORTEP diagram of compound **3** with thermal displacement parameters drawn at the 30% probability level. Selected bond lengths [Å] and bond angles [°]: O(1)-C(18) 1.422(4), O(1)-H(1) 0.91(7), O(2)-C(25) 1.436(4), O(2)-H(2) 0.86(5), N(1)-C(1) 1.379(4), N (1)-C(11) 1.460(4), N(2)-C(7) 1.404(4), N(2)-C(7) 1.404(4), C(18)-O(1)-H (1)94(4), C(25)-O(2)-H(2)108(3), C(1)-N(1)-C(11) 120.2(3), C(1)-N(1)-H (5) 119.9, C(11)-N(1)-H(5) 119.9, C(7)-N (2)-C(11) 116.9(3), N(1)-C(11)-N(2) 107.0(3), N(3)-C(32)-C(25) 111.2(3), N(4)-C(32)-C(25) 106.0(3), O(2)-C(25)-C(32) 106.7(3), O(1)-C(18)-C(19) 109.3(3), O(1)-C(18)-C(11) 111.0(3), O(2)-C(25)-C(26) 111.0(3), N(1)-C(11)-C(18) 107.4(3), N(2)-C(11)-C(18) 110.0(3), N (3)-C (32)-N(4) 106.9(3), N(3)-C(32)-C(33) 112.2(3), N(4)-C(32)-C(33) 113.2(3)

be assigned to the resonance of the amine protons (5.03), which are slightly high field shifted when compared to compound **2** (5.22), alcoholic proton (3.22) and methine proton (4.95). The aromatic protons in compound **3** are in the expected regions. In FT-IR spectra of compound **3**, the characteristic absorption band appeared at ν = 3350 cm^{-1} for –OH group and ν = 3215 cm^{-1} for two –NH groups, which also confirm the formation of compound **3** by reduction of compound **2**.

The solid-state structures of compounds **2** and **3** were established using single-crystal X-ray diffraction analysis. Compound **2** crystallizes in the monoclinic space group $P2_1/n$ having four independent molecules in the unit cell (see Figure 1). Compound **3** crystallizes in the triclinic space group *P* -1 having four independent molecules in the unit cell (see Figure 2). The details of the structural parameters for compounds **2** and **3** are given in Table 1. In compound **2**, the C18–O1 bond distance of 1.217(3) Å is within the range of the typical carbonyl C=O bond (1.22 Å), C–N bond distances observed

ISSN 2291-6458 (Print), ISSN 2291-6466 (Online)
Year 2014 | Volume 2 | Issue 1 | Page 72-82

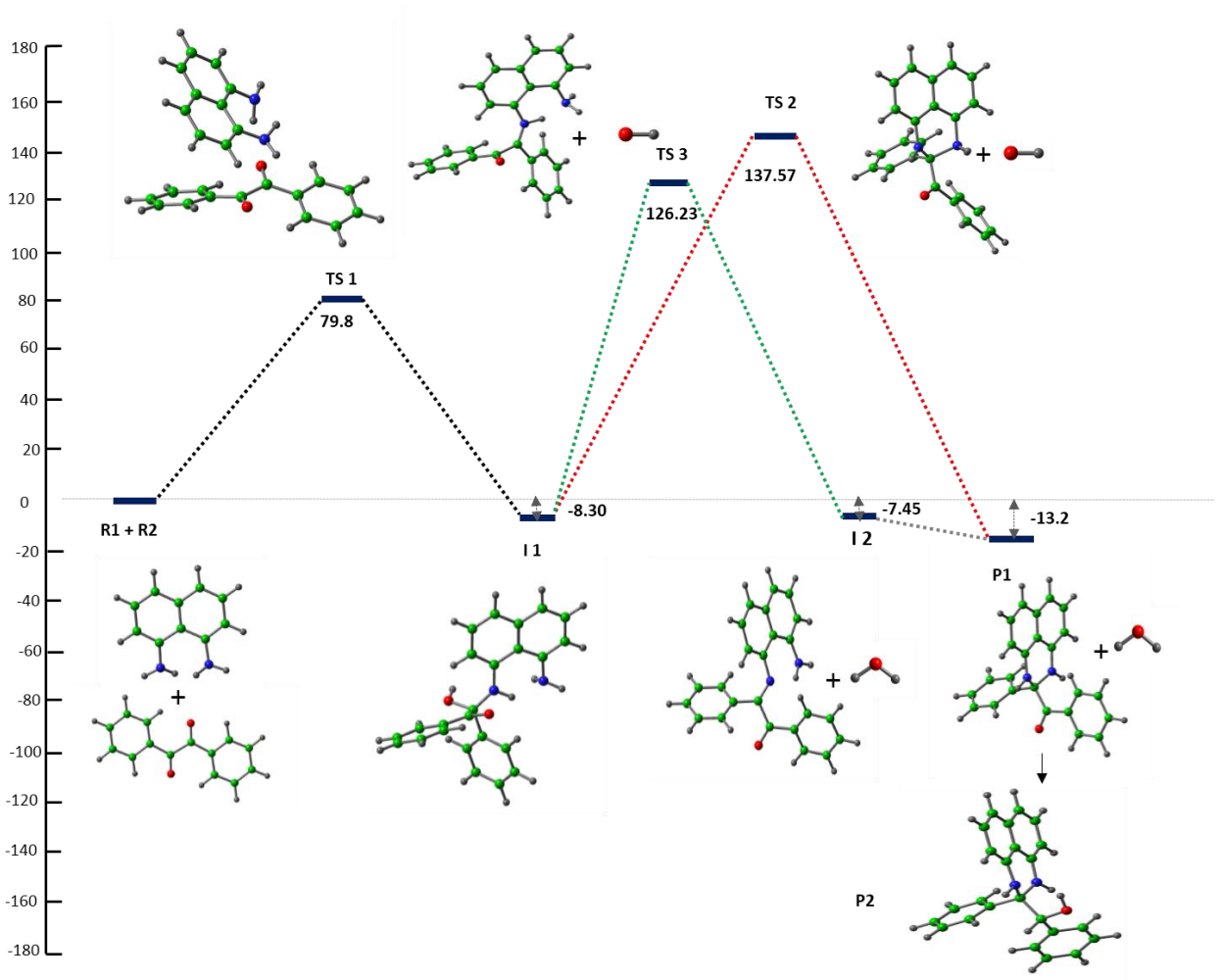

Figure 3. Reaction mechanism scheme: optimized structures of different transition states and intermediates. The red dotted line denotes mechanism pathway 1 and green dotted line denotes mechanism pathway 2. The relative energy values are shown in kcal/mol. The black dotted line is common to both pathways

from 1.39º(2) Å to 1.470(2) Å is in agreement with amine bond lengths. In compound **2**, both nitrogen atoms N1 and N2 are almost coplanar with the aromatic ring, having a dihedral angle of 3.19º. However, atom C1 resides 0.638 Å above the mean plane containing N1, C10, C11, C2 and N2 atoms. An intramolecular hydrogen bonding between H16 and the carbonyl oxygen (H....O = 2.666 Å) is observed. In compound **3**'s solid-state structure, two molecules of compound **3** are present in the asymmetric unit. The C18–O1 bond distance of 1.422(4) Å confirms the carbon–oxygen single bond, with a much-elongated carbonyl bond (1.217(3) Å) observed in compound **2**. Intermolecular hydrogen bonding H5...O2 (2.112 Å) is observed between the NH proton of the first molecule and the oxygen atom of second molecule. Another hydrogen (OH) group is μ_2 bridged (H1...O2 2.075 Å) between the oxygen atom and (H1....N4 2.358 Å) the nitrogen atom of the adjacent molecule. Similar to compound **2**, in compound **3**, both the nitrogen atoms N1 and N2 (N3 and N4 for molecule **2**) are almost coplanar with the aromatic ring, having a dihedral angle of 4.74º (3.90º for molecule **2**). The C11 (C32 for molecule **2**) sits 0.535 Å (0.57 Å for molecule **2**) above the average plane containing the nitrogen atoms and the aromatic rings. A dihedral angle of 73.23º (83.24º for molecule **2**) is observed between the plane O1, C18, C11 and

ISSN 2291-6458 (Print), ISSN 2291-6466 (Online)
Year 2014 | Volume 2 | Issue 1 | Page 72-82

the average plane containing nitrogen atoms and aromatic rings.

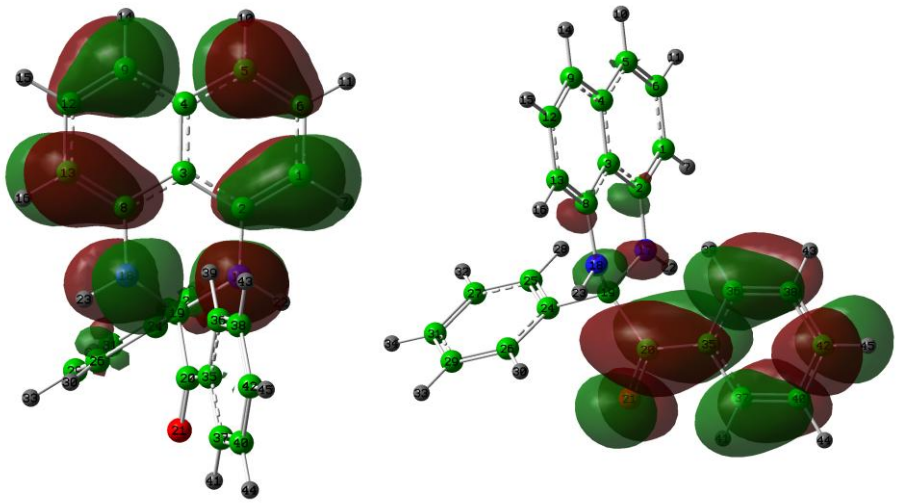

Figure 4. Pictures of HOMO and LUMO of product **P1**. The HOMO-LUMO gap is -2.48 eV

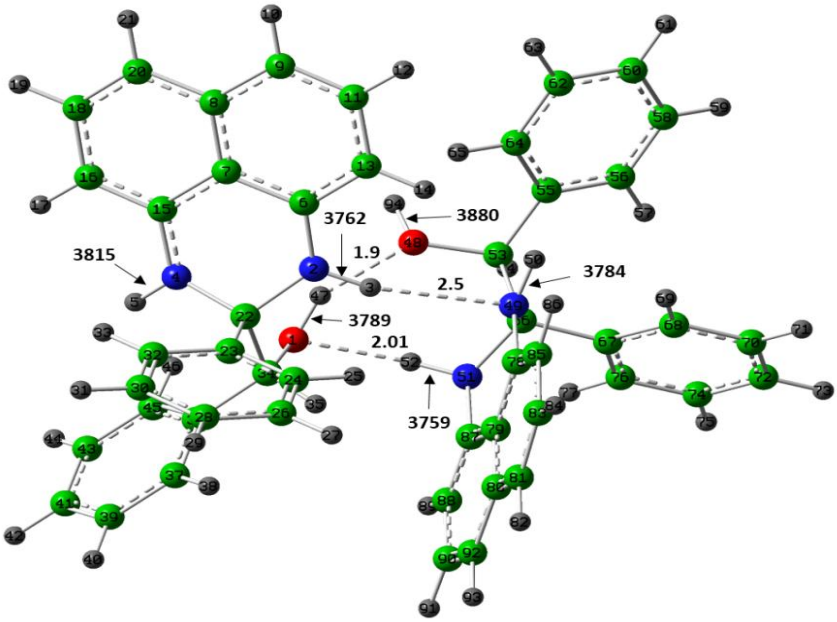

Figure 5. Optimized geometry of dimeric compound **3**. All frequencies and hydrogen bond distances are shown in cm^{-1} and Å units, respectively

ISSN 2291-6458 (Print), ISSN 2291-6466 (Online)
Year 2014 | Volume 2 | Issue 1 | Page 72-82

3.2. DFT Analysis

In the DFT calculations, we explored two possible reaction mechanism pathways designated by red and green dotted lines. Both the reaction mechanism pathways initially pass through a common transition state (**TS1**) and intermediate state (**I1**). The formation of **TS1** takes place through the lone pair attack by one of the nitrogen atoms of **R1** on the carbonyl carbon of **R2**. The nearest N–C and O–H bond distances are found to be 2.94 Å and 3.13 Å respectively for **TS1**. The interaction between the participating amine and carbonyl groups leads to the formation of a N–C covalent bond and proton transfer by forming **I1**; the relative stabilization energy of this intermediate is -8.30 kcal/mol with respect to **R1** and **R2**. Now, based on the availability of a lone pair of nitrogen atoms, the reactions can progress in either of the proposed ways. Both the proposed paths contain elimination of OH- in their transition states: **TS2** and **TS3**, but the former path, having lower energy, is formed due to the attack of a lone pair of the same nitrogen atoms on the carbon-centre-bearing OH group, while the latter involves the attack of a lone pair from the far amino group, which is not so favourable, energy-wise. In the next step, water is eliminated and thus product **P1** is formed from **TS2**. The pathway also contains elimination of the water molecule by forming **I2**, followed by the lone pair attack by other nitrogen atoms to the carbon centre of C=N bond to form **P1**. We also calculated the HOMO–LUMO energy gap for this product and orbital pictures are shown in Figure 4. In **P1**, electron density in HOMO is on naphthalene and two –NH groups. The electronic structure analysis of **P1** explains the charge transfer interactions and most of the electron density transfer from naphthalene and –NH moieties to Ph–CO moiety.

From the experiment, **P1** is not the final product. After reduction of **P1** by sodium borohydride followed by acid treatment, the monomeric product **P2** is formed, which undergoes dimerization; dimeric structure was confirmed by the crystal structure. The stabilization energy of **P2** is found to be – 441 kcal/mol with respect to **P1**. We also carried out energy calculations to understand the stability of the dimer (see Figure 5). It was found that the stability of the dimer comes from the existence of three types of hydrogen-bonding pairs: O-H--O, O-H--N and N-H--N, which are absent in the monomer. The monomer contains free or non-hydrogen bonded O–H and N–H groups, whereas the dimer contains both free and hydrogen bonded ones. We conducted a vibrational frequency analysis to understand the hydrogen bonding nature of these groups in comparison to non-hydrogen bonded ones. The various hydrogen-bond distances and frequencies are shown in Figure 5. In the dimer complex, the values of hydrogen bonded –X-H (X = O, N) stretching frequencies are lower than the free –X-H groups of same complex and also of the monomer. The frequencies of free groups in the dimer complex are very close to that of the monomer.

4. CONCLUSIONS

In summary, we have presented the synthesis and structural characterization of two perimidines, phenyl(2-phenyl-2,3-dihydro-1H-perimidin-2-yl)methanone and phenyl(2-phenyl-2,3-dihydro-1H-perimidin-2-yl)methanol in the absence of any catalyst. We have also performed DFT calculations to confirm the mechanism of formation of perimidines by the reactions of 1,8-diaminonaphthalene and benzyl. The optimized structure of phenyl(2-phenyl-2,3-dihydro-1H-perimidin-2-yl)methanol (dimer) shows excellent agreement with its solid-state structure established by single-crystal analysis. Currently we are in the process to explore the coordination behaviour of various perimidines and their derivatives into transition metal chemistry.

ACKNOWLEDGEMENTS

This work was supported by the Department of Science and Technology, Ministry of Science and

ISSN 2291-6458 (Print), ISSN 2291-6466 (Online)
Year 2014 | Volume 2 | Issue 1 | Page 72-82

Technology, Government of India (DST) under the SERC Fast Track Scheme (SR/FT/CS-74/2010) and start-up grant from Indian Institute of Technology Hyderabad to TKP and BSM. SA thanks CSIR, India for his PhD fellowship.

REFERENCES AND NOTES

[1] A. E. A. Porter, "Comprehensive Heterocyclic Chemistry" ed. By A. R. Katritsky, C. W. Ress., *Pergamon Press, Oxford*, **1984**.
[2] Pozharskii, A. F.; Dalnikovskaya, V. V. Perimidines, *Russ. Chem. Rev*. **1981**, *50*, 816–835;
[3] Liu, K. C. Zhonghua Yaoxue Zazhi **1988**, *40*, 203–216;
[4] Claramunt, R. M.; Dotor, J.; Elguero, Structure, reactivity, and synthesis of perimidines and their derivatives (dihydroperimidine and perimidinones) *J. Ann. Quim.* **1995**, *91*, 151–183;
[5] Undheim, K.; Benneche, C. In Comprehensive Heterocyclic Chemistry II; Katritzky, A. R., Rees, C. W., Scriven, E. F. V., Eds.; Pergamon Press, Oxford, 1996.
[6] Woodgate, P. D.; Herbert, J. M.; Denny, W. A. The Preparation of Pyrido[4,3,2-de]quinazoline and Pyrido[3,4,5-de]quinazoline, *Heterocycles* **1987**, *26*, 1029–1036.
[7] Bazinet, P.; Yap, G. P. A.; Richeson, D. S. Constructing a Stable Carbene with a Novel Topology and Electronic Framework *J. Am. Chem. Soc*. **2003**, *12*5, 13314–13315.
[8] Herbert, J. M.; Woodgate, P. D.; Denny, W. A. Potential antitumor agents. 53. Synthesis, DNA binding properties, and biological activity of perimidines designed as minimal DNA-intercalating agents, *J. Med. Chem*. **1987**, *30*, 2081–2086.
[9] Bu, X.; Deady, L. W.; Finlay, G. J.; Baguley, B. C.; Denny, W. A. Synthesis and Cytotoxic Activity of 7-Oxo-7H-dibenz[f,ij]isoquinoline and 7-Oxo-7H-benzo[e]perimidine Derivatives, *J. Med. Chem*. **2001**, *44*, 2004–2014.
[10] Mobinikhaledi, A.; Amrollahi, M. A.; Foroughifar, N.; Jirandehi, H. F. Microwave Assisted Synthesis of Some 2-Alkyl and 2-Arylperimidines, *Asian J. Chem.* **2005**, *17*, 2411–2414.
[11] Mobinikhaledi, A.; Foroughifar, N.; Goli, R. Synthesis of Some Benzotriazole-Substituted Perimidines, *Phosphorus, Sulfur Silicon Relat. Elem*. **2005**, *180*, 2549–2554.
[12] A. Shaabani, A. Maleki, Green and Efficient Synthesis of Quinoxaline Derivatives via Ceric Ammonium Nitrate Promoted and in Situ Aerobic Oxidation of α-Hydroxy Ketones and α-Keto Oximes in Aqueous Media, *Chem. Pharm. Bull*. **2008**, *56*, 79-81.
[13] A. Mobinikhaledi, N. Foroughifar, N. Basaki, Zeolite catalyzed efficient synthesis of perimidines at room temperature, *Turk J Chem*, **2009**, *33*, 555 – 560.
[14] I. A. S. Smellie, A. Fromm, R. M.Paton, A new route to 2-substituted perimidines based on nitrile oxide chemistry, *Tetrahedron Letters*, **2009**, *50*, 4104–4106.
[15] R. M. Claramunt, J. Dotor, D. Sanz, C. F-Foces, A. L. L-Saiz, and J. Elguero, R. Flammang, J. P.Morizur, E.Chapon, J. Tortajada, The Structure of 1H-Perimidin-2(3H)-one and Its Derivatives in the solid state (x-ray crystallography and CP/MAS ^{13}C-NMR), in solution (^{13}C-NMR), and in the gas phase (mass spectrometry) (pages 121–139), Helvetica Chimica Acta, **1994**, *77*, 121-139.
[16] M. H. Ghorbani, 2-Methylsulfanyl-1H-perimidin-3-ium iodide, *Acta Crystallographica Section E*, **2012**, *E68*, o2605.
[17] M. Sheldrick SHELXS-97, Program of Crystal Structure Solution, University of Göttingen, Germany, **1997**.
[18] G. M. Sheldrick SHELXL-97, Program of Crystal Structure Refinement, University of Göttingen, Germany, **1997**.

ISSN 2291-6458 (Print), ISSN 2291-6466 (Online)
Year 2014 | Volume 2 | Issue 1 | Page 72-82

[19] Gaussian 09, Revision B.01, M. J. Frisch, G. W. Trucks, H. B. Schlegel, G. E. Scuseria, M. A. Robb, J. R. Cheeseman, G. Scalmani, V. Barone, B. Mennucci, G. A. Petersson, H. Nakatsuji, M. Caricato, X. Li, H. P. Hratchian, A. F. Izmaylov, J. Bloino, G. Zheng, J. L. Sonnenberg, M. Hada, M. Ehara, K. Toyota, R. Fukuda, J. Hasegawa, M. Ishida, T. Nakajima, Y. Honda, O. Kitao, H. Nakai, T. Vreven, J. A. Montgomery, Jr., J. E. Peralta, F. Ogliaro, M. Bearpark, J. J. Heyd, E. Brothers, K. N. Kudin, V. N. Staroverov, T. Keith, R. Kobayashi, J. Normand, K. Raghavachari, A. Rendell, J. C. Burant, S. S. Iyengar, J. Tomasi, M. Cossi, N. Rega, J. M. Millam, M. Klene, J. E. Knox, J. B. Cross, V. Bakken, C. Adamo, J. Jaramillo, R. Gomperts, R. E. Stratmann, O. Yazyev, A. J. Austin, R. Cammi, C. Pomelli, J. W. Ochterski, R. L. Martin, K. Morokuma, V. G. Zakrzewski, G. A. Voth, P. Salvador, J. J. Dannenberg, S. Dapprich, A. D. Daniels, O. Farkas, J. B. Foresman, J. V. Ortiz, J. Cioslowski, and D. J. Fox, Gaussian, Inc., Wallingford CT, 2010.

[20] GaussView, Version 5, Roy Dennington, Todd Keith and John Millam, *Semichem Inc*., Shawnee Mission KS, 2009.

[21] (a) A. D. Becke, Density-functional thermochemistry. III. The role of exact exchange *J. Chem. Phys*, **1993**, 98, 5648. (b) C. Lee, W. Yan, R. G. Parr, Development of the Colle-Salvetti correlation-energy formula into a functional of the electron density, *Phys. Rev. B*. **1988**, 37, 785.

[22] J.B. Foresman and T. M. Frisch, Exploring Chemistry with Electronic Structure Methods, Second Edition, Gaussian, Inc. Pittsburgh, PA

The authors declare no conflict of interest

© 2014 By the Authors; Licensee Borderless Science Publishing, Canada. This is an open access article distributed under the terms and conditions of the Creative Commons Attribution license http://creativecommons.org/licenses/by/3.0/